Comparative Study of Analytical and Simulated Doubly-Supported RF MEMS Switches for Mechanical and Electrical Performance

Nickolas Kingsley, Guoan Wang, and John Papapolymerou
E-mail: Kingsley@gatech.edu, gtg647e@prism.gatech.edu, papapol@ece.gatech.edu

Georgia Institute of Technology, School of Electrical and Computer Engineering, Atlanta, GA 30308

***Abstract* — Radio Frequency Microeletromechanical System (RF MEMS) switches are useful for providing low-loss switching elements in high frequency devices. Since these devices contain a mechanical and an electrical component to their operation, predicting their performance is not trivial. Computational analysis can be extremely complicated due to the large number of variables that need to be incorporated. Using a multi-physics simulation tool seems like the only solution, but most simulators are optimized for only one engineering realm (i.e. mechanics or electronics). Combining different engineering realms into one simulated model will usually compromise the accuracy of the results. Often simulators cannot model a multi-realm device at all. This paper offers a solution to this problem by proposing a technique for combining computational analysis with simulation to determine the pull-down voltage and RF characteristics of an RF MEMS switch. Measurement results agree closely with the simulated results using this technique.**

I. INTRODUCTION

RF MEMS switches have become a popular area of research in recent years due to their small size, low loss, good isolation, and low cost. Solid-state switches at high frequencies are lossy and cause more distortion. An example of a doubly-supported (air-bridge type) capacitive MEMS switch is shown in Figure 1.

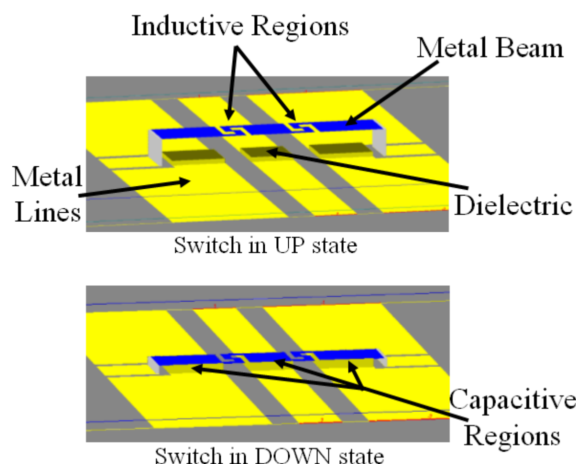

Fig. 1. Rendering of RF MEMS switch in UP and DOWN state.

The switch works by deflecting the beam towards the bottom metal layer and causing an RF short circuit. The inductive regions behave like springs and make it easier to deflect the beam. A spring constant can be determined which evaluates the amount of force necessary to deflect the beam a given distance. Changing the shape or dimensions of the inductive region will increase or decrease the spring constant. The capacitive regions are responsible for creating an electrostatic force between the DC biased beam and the metal layer below it. This force is responsible for decreasing the "gap" between the metal layers. Changing the gap length, height, or the area of the capacitive region will increase or decrease the electrostatic force necessary to deflect the beam.

Across the capacitive region, the charge density in the metal should be uniform. Otherwise, the beam will not deflect parallel to the bottom metal layer. Any skewing of the beam caused by fabrication misalignment or non-symmetric inductive regions will result in a larger capacitance and a poor RF open circuit. As long as the switch is adequately thick (2-3 skin depths), made from a high-quality, highly conductive metal (copper or gold, usually), and properly aligned (to equalize the fringing electric fields on all sides) charge density in the metal will be uniform. MEMS switches that are not deflecting uniformly are usually caused by fabrication misalignment, non-uniform metal thickness, or contaminants in the capacitive region metal. The latter two issues prevent the charge density from being uniform by hampering the flow of electrons in the metal and can be rectified by altering the fabrication recipe.

Electrically, the inductive and capacitive regions behave as their name implies. Changes in these regions will change the RF performance of the switch. The dielectric layer provides high capacitance when the switch is in the down state and is used to prevent stiction between the two metal layers. A very thin layer (~2000Å) of silicon nitride is typically used and generally has a negligible effect on the mechanics of the switch. That is, the bending of the beam is not directly effected by the presence of the silicon nitride. However, electrons can accumulate in this thin layer which can build up a large enough charge to effect the electrostatic actuation of the switch. Dielectric charging is especially pronounced in silicon nitride layers that are deposited using Plasma

Enhanced Chemical Vapor Deposition (PECVD) because of the large number of atomic defects generated from the plasma. Charging effects can be greatly reduced by properly grounding the silicon nitride to prevent electron accumulation. This can be improved further by thermally growing the dielectric layer instead of using PECVD [1].

Modeling MEMS switches for optimal electrical and mechanical performance can be a daunting task and is often substituted with a less accurate method. For instance, MEMS switches are often designed for optimal electrical properties (such as a low RC time constant [2]) or optimal mechanical properties (such as a low actuation voltage [3]). There are four popular inductive region configurations [4]. These designs, labeled 1-4, are shown in Figure 2.

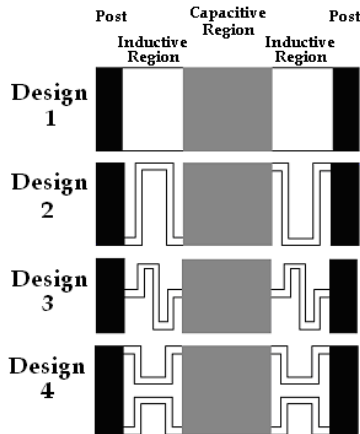

Fig 2. Switch designs 1-4.

Deriving the equations for predicting MEMS switch performance that utilizes these inductive and capacitive regions is difficult. Very general equations can be investigated but the results can only be used as rough estimates [5-6]. Those who have tried predicting MEMS switch behavior using only theory often report a discrepancy upwards of a factor of ten between predicted and measurement results [7]. Certainly design optimization can not be done this way. Using simulation software is the only way to take into account most of the idiosyncrasies of device performance. However, it is not always possible, or effective, to use a simulator to predict mechanical performance due to an electrostatic force.

RF MEMS switch feature sizes are often on the order of λ/1000 or smaller. This is much smaller than the typical element size of a Finite Element Method (FEM) or Finite-Difference Time-Domain (FDTD) simulator, whose typical element sizes are λ/20 to λ/10, although simulations with small feature sizes are still possible with these methods [8]. A Method of Moments (MOM) simulator could be used to model the small feature sizes, but if the switch is being simulated with other devices (i.e. filters or antennas) or on a multilayer substrate then an FEM simulator would be more accurate because of the improved cell size. Clearly there is a trade off. Alternatively, hybrid simulators have been investigated which attempt to utilize the advantages of both types of simulation. No matter which type of simulator is used, when devices with small feature sizes (i.e. RF MEMS switches) are simulated in a complex environment (i.e. when surrounded by an electric field) assumptions must be made within the simulator and results will be compromised [9].

Often, when multiple physical realms are involved in a problem, the optimal solution method is to use a simulator to solve the problem in the more complicated realm and to combine those results manually with theory from the simpler realm. For the RF MEMS switch, we are combining a mechanical beam dynamics problem with an electrostatic problem. The theory that deals with the electrostatics of a capacitive region is well known and straightforward, whereas the dynamics of a beam with complicated springs is much more difficult to solve. Solving the problem in one simulation that couples the two physical realms does not always give the most accurate results because of assumptions and simplifications used in the simulator. Instead, this paper presents a straightforward method for modeling an RF MEMS switch by simulating first in an optimized FEM mechanical simulator then calculating the pull-down voltage by using simple electrostatic equations. The measured results match very closely with the results from this method, which demonstrates its effectiveness.

II. MECHANICAL ANALYSIS OF RF MEMS SWITCHES

Equations for predicting the bending of cantilever and doubly-supported beams have been around for decades [10]. Unfortunately, applying simplistic equations to complex MEMS devices can be cumbersome. The two most important mechanical features of a MEMS switch are the pull-down voltage and the deflection. Both of these quantities can be calculated by treating the MEMS switch as a mechanical spring. In order to calculate the pull-down voltage, one must equate the force pulling down on the beam by the electrostatic force between the metal layers

$$f_{down} = \frac{\varepsilon A V^2}{2g^2} \tag{1}$$

and the force pushing up from the spring (Hooke's Law) [11],

$$f_{up} = -k(g_o - g)\,. \tag{2}$$

For these equations, ε is the permittivity, A is the area, V is the voltage, k is the spring constant, g_o is the initial gap, and g is the evaluated gap. We can use these simple, spatially independent equations since we know the charge density (and therefore the force) is uniform across the capacitive region. It has been well documented that for parallel plate electrostatic actuation, when the gap reduces to 2/3 of the original gap, the beam becomes unstable and experiences a "pull-in" effect [11]. That is, the MEMS switch does not deflect over the entire gap according to the formula in (1). Instead, when the gap

reaches a certain threshold, namely 2/3 the original gap, the switch will snap down. Magnets experience the same effect. As two magnets of opposite polarity are brought closer together the attractive force is barely noticeable until they reach a certain distance apart. At this point they snap together and the force between them is great.

Equating (1) and (2) where the gap is 2/3 the original gap and solving for the pull down voltage gives

$$V_{PI} = \sqrt{\frac{8kg_o^3}{27\varepsilon A}}\,. \tag{3}$$

The maximum deflection can also be calculated from the spring constant by the equation [10]

$$\delta = {-F}/{k} \tag{4}$$

where δ is the deflection, F is the force pushing down on the spring (in Newtons) and k is the spring constant.

The values for the permittivity, area, and gap can be designed for and implemented in fabrication. The only two unknowns for a given MEMS switch are the spring constant and the downward force. The spring constant can be derived for a meandered line by the equation [4]:

$$k_m = \frac{Ew\left(\frac{t}{L_c}\right)^3}{1+\frac{L_s}{L_c}\left(\left(\frac{L_s}{L_c}\right)^2+12\frac{1+\nu}{1+\left(\frac{w}{t}\right)^2}\right)} \tag{5}$$

where w is the width of the meander, t is the thickness of the metal, v is the Poisson's Ratio of the metal, L_s is the overall width of the spring, and L_c is the distance from the end of the spring to the start of the meander. These dimensions are illustrated below.

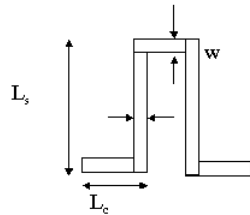

Fig.3. Illustration of dimensions for (5).

For a non-meandered spring, the spring constant is given by [12]

$$k_{non-m} = \frac{32EWH^3}{L^3} \tag{6}$$

where E is the Young's Modulus, W is the width, H is the thickness, and L is the length.

The effective spring constant, k_{eff}, for the entire MEMS switch can be determined by combining the simple spring equations in a fashion similar to capacitors. That is, springs in parallel add directly and springs in series add as the inverse of the sum of the reciprocals. Therefore, the effective spring constants for the four switch designs presented in this paper are:

Design 1

$$k_{eff} = \frac{32EWH^3}{L^3} \tag{7}$$

Design 2

$$\frac{1}{k_{eff}} = \frac{1}{k_m} + \frac{1}{k_{n-m}} + \frac{1}{k_m}$$

$$\therefore k_{eff} = \frac{k_m k_{n-m}}{k_m + 2k_{n-m}} \tag{8}$$

Design 3

$$\frac{1}{k_{eff}} = \frac{1}{k_m} + \frac{1}{k_m} + \frac{1}{k_{n-m}} + \frac{1}{k_m} + \frac{1}{k_m}$$

$$\therefore k_{eff} = \frac{k_m k_{n-m}}{k_m + 4k_{n-m}} \tag{9}$$

Design 4

$$\frac{1}{k_{eff}} = \frac{1}{2k_m} + \frac{1}{k_{n-m}} + \frac{1}{2k_m}$$

$$\therefore k_{eff} = \frac{k_m k_{n-m}}{k_m + k_{n-m}} \tag{10}$$

where k_m is the meandered spring constant given by (5) and k_{n-m} is the non-meandered spring constant given by (6). Substituting k_{eff} from (7)-(10) into (3) for k will give the theoretical pull down voltages.

III. MECHANICAL SIMULATION OF RF MEMS

Before any complex mechanical simulations are performed, it is necessary to validate the model. Careful attention must be given to material properties, boundary conditions, and the applied forces. One way to validate a simulation model is to compare simulated values with theoretical values for a simple case. If the results agree, more complicated configurations can be simulated and the results can be trusted.

A. Verification of Simulation Tool

The FEMLAB 3.0 static structural mechanics module from Comsol was used for the mechanical simulations. FEMLAB is a multiphysics simulation tool, which is commonly used in industry and university settings [13]. The 3D MEMS switch structure with non-meandered springs (Design 1) was simulated with a uniform force pushing down on the center capacitive region.

The theoretical deflection profile can be determined by taking advantage of spring superposition. This procedure

is demonstrated in the figure below for the distribution of force, q.

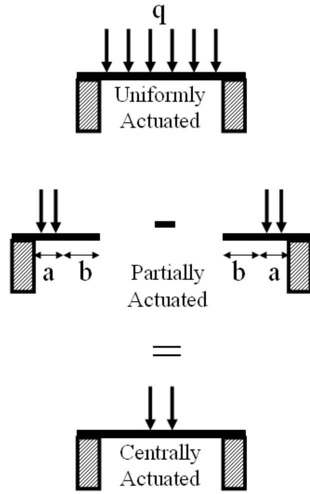

Fig. 4. Spring superposition.

The deflection equation for a uniformly actuated beam is given by [10]

$$\delta(x) = \frac{x^2\left(L^2 - 2Lx + x^2\right)q}{2EWH^3} \quad (11)$$

where x is the position along the beam, L is the length of the beam, and q is the force applied per length. These parameters are exemplified in Figure 5.

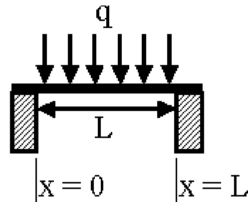

Fig. 5. Illustration of dimensions for (11).

The deflection equation for a partially actuated beam is given by [11]:

$$\delta = \begin{cases} -\dfrac{qbx^2}{12EI}\left(3L + 3a - 2x\right) & \text{for } 0 \le x \le a \\ -\dfrac{q}{24EI}\left(x^4 - 4Lx^3 + 6L^2x^2 - 4a^3x + a^4\right) & \text{for } a \le x \le L \end{cases} \quad (12)$$

where a is the distance from the anchor that the force begins, b is the length of the beam that the force is applied to, and I is the moment of inertia given by [12]:

$$I = \frac{HW^3}{12} \quad (13)$$

where H is the thickness and W is the width of the beam. Figure 6 shows a plot of the deflection given by FEMLAB and the results from the superposition of (11) and (12).

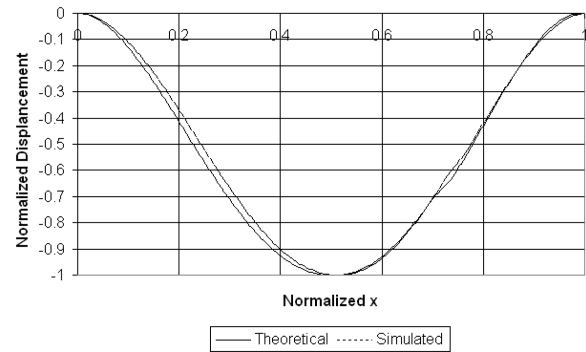

Fig. 6. Comparison of Simulated and Analytical displacement of non-meandered switch.

Since the simulation results agree closely with the analytical results, it is safe to assume that the simulator will be reasonably accurate for the more complicated spring configurations. The simulated deflection profile of the four switch designs is shown in Figure 7.

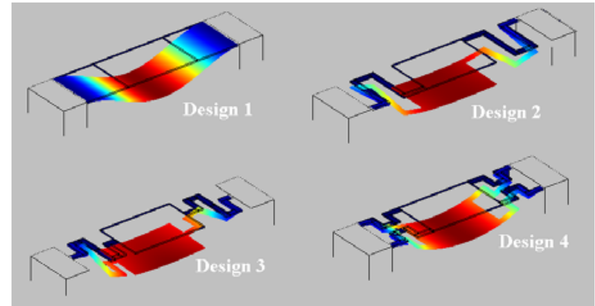

Fig.7. 3D Deflection Profile of RF MEMS Switches.

B. Deriving Pull-down Voltage from Simulation

Using FEMLAB, it is easy to determine the force necessary to deflect the MEMS switch a desired distance. Ideally, it is necessary to deflect the MEMS switch the same distance as the gap between the beam and the metal layer below it (usually 1.5-3μm). The equation that relates force to pull-down voltage in terms of the gap is given by [10]

$$V_{PI} = \sqrt{\frac{2g^2F}{\varepsilon}} \quad (14)$$

where F is the force per area. This equation is derived from the pull-down voltage in (3), where F incorporates the spring constant. Doing a unit analysis between (3) and (14) will result in the same outcome, volts.

Changing the force per area acting on the capacitive region until the deflection matches the gap will determine the force. Although a guess-and-check method is necessary to determine the value, this can be performed quickly using interpolation since force and deflection are linearly related. This force can then be used in (14) to calculate the pull-down voltage.

IV. ELECTRICAL SIMULATION OF RF MEMS

In addition to the mechanical performance of MEMS switches, it is important to evaluate the RF characteristics. The springs exhibit an inductance, the actuation region exhibits a capacitance, and the metal beam exhibits a resistance. All together, the beam behaves like a series RLC circuit. These values can be calculated within an order of magnitude by using fundamental RLC equations. The resistance can be calculated using [14]:

$$R = \frac{\rho L}{HW} \quad (15)$$

where ρ is the metal resistivity and L is the length of the beam. The capacitance can be calculated using [14]:

$$C = \frac{\varepsilon A}{g} \quad (16)$$

Knowing the resonant frequency from measurements, the inductance can be calculated using [14]:

$$L = \frac{1000}{4\pi^2 C f^2} \quad (17)$$

where f is the resonant frequency given in GHz, C is given in pF, and L is calculated in nH. Papers have been published which investigate elaborate circuit models for MEMS switches [15-16]. However, if results within an order of magnitude are suitable, these simple equations are more than adequate.

V. MEASUREMENTS

All four switch designs were fabricated and measured to determine the actual pull-down voltage and resonance frequency. The process steps are shown in Figure 8. The coplanar waveguide (CPW) signal lines were fabricated by electron beam evaporating a titanium – gold (Ti-Au) layer. Silicon nitride (Si_3N_4) was deposited using Plasma Enhanced Chemical Vapor Deposition (PECVD) and patterned using a Reactive Ion Etch (RIE). A sacrificial photoresist layer was spun on and hard baked. The sacrificial layer was removed using a photoresist stripper and a carbon dioxide (CO_2) critical point drying process was used to release the switches.

Scanning electron pictures of two of the switches are shown in Figure 9.

Measurements were taken with Thru-Reflect Line (TRL) calibration to deembed the cable and connector losses.

VI. RESULTS

Results for the mechanical and electrical characteristics of the four spring designs are presented in the following sections. Measurement results were taken for each design. The measured pull-down voltage is within 5V of the minimum pull-down voltage. Voltage ramping must be done quickly to minimize charge accumulation in the underlying dielectric region.

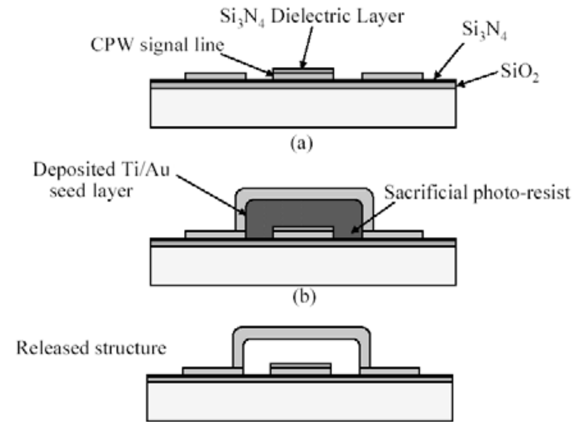

Fig. 8. Fabrication process for MEMS switches.

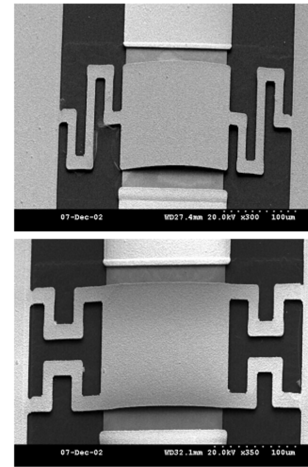

Fig. 9. SEM photos of fabricated switches.

A. Comparison of Mechanical Analysis

Table 1 displays the comparison between the purely theoretical, the simulated method presented in this paper, and the measured pull-down voltage.

TABLE I
COMPARISON OF THEORETICAL, SIMULATED, AND MEASURED VPI

Design	Theoretical	Simulated	Measured	Avg Error	Avg % Error
1	117.135V	127.5V	100V	13.75	11.97%
2	40.547V	38.4V	35V	3.85V	10.14%
3	31.875V	27.8V	30V	2.98V	9.97%
4	69.050V	72.8V	70V	2.35V	3.33%

The measurement results agree closely with the theoretical and simulated results. The average error is within the measurement ramping tolerance (5V).

The theoretical results are generally within 5-8% of the simulated values. The small discrepancy is mainly due to the Poisson ratio of the metal, which the simulator takes into account and theory does not [10,13]. The Poisson ratio relates a change in the width as the length of the beam is increased. There is a small discrepancy between

simulated and theoretical values due to simulator meshing tolerances.

B. Comparison of Electrical Analysis

The switches were measured to determine the resonance frequency. This is shown in the figure below.

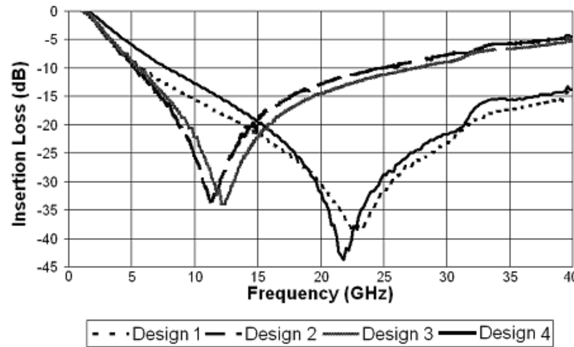

Fig. 10. Resonance frequency of MEMS switches.

Using the measured resonance frequency and the capacitance calculated from (16), the inductance can be determined by (17). The resistance can be calculated from (15). Table 2 shows the resonance frequency values and the calculated capacitance, inductance, and resistance.

TABLE II
CAPACITANCE, INDUCTANCE, AND RESISTANCE OF RF MEMS

Design	Resonant Frequency	C	L	R
1	22.8175GHz	2.2pF	22pH	0.3Ω
2	11.3625GHz	2.9pF	65pH	0.6Ω
3	12.1525GHz	2.8pF	60pH	0.5Ω
4	21.83GHz	1.9pF	28pH	0.2Ω

The measurement results were compared to a series RLC circuit with the same values as Table 2 to verify the model. One such comparison is shown in Figure 11.

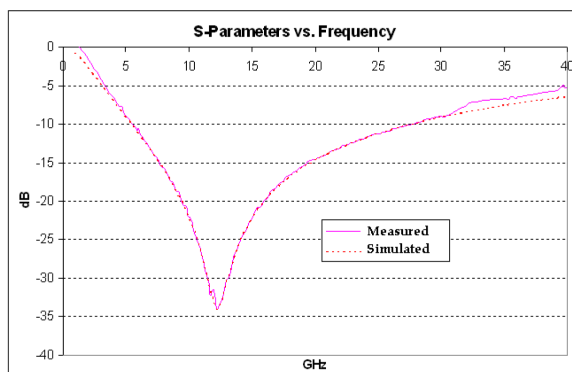

Fig. 11. RLC Circuit vs. Measurement Results.

These results agree very closely with each other. The electrical model is satisfactory.

VII. CONCLUSION

In this paper, four different RF MEMS switch designs were analyzed using theory and simulations. By combining mechanical simulation results with simple electrostatic equations, a prediction for the pull-down voltage and RF performance was achieved. This prediction was more accurate and much easier to determine than using only theory or only simulations. To verify our mechanical simulation model, it was shown that for a simple switch geometry, the simulated deflection closely matched the theoretical displacement found by using spring superposition. A pull-down voltage for each switch was determined by using the pull-down force given by the mechanical simulator with an equation that relates force to voltage. Measuring the resonant frequency and calculating the resistance, capacitance and inductance determined the electrical circuit model. These RLC values can be used to design other RF MEMS switches. Measurement results agreed very well with predicted values, thus demonstrating that simulation results can be conveniently combined with analytical results to achieve accurate predictions.

ACKNOWLEDGEMENT

The authors wish to thank Holly Kingsley for her insight on the mechanics of springs and for verifying this paper from a mechanical engineering perspective. The authors would also like to thank Dr.Oliver Brand for inspiring this project.

This work is partially supported by GEDC and partially by NASA under contract #NCC3-1057.

REFERENCES

[1] Campbell, Stephen, "The Science and Engineering of Microelectronic Fabrication, Second Edition" Oxford University Press, 2001.

[2] S. Simion, "Modeling and design aspects of the MEMS switch," *Semiconductor Conference*, vol. 1, pp. 128, Oct. 2003.

[3] Pacheco, S.P.; Katehi, L.P.B.; Nguyen, C.T.-C., "Design of low actuation voltage RF MEMS switch," *IEEE MTT-S Microwave Symposium Digest*., vol. 1, pp. 165-168, June 2000.

[4] Wang, G., Barstow, S., Jeyakumar, A., Papapolymerou, J., Henderson, C., "Low cost RF MEMS switches using photodefinable mixed oxide dielectrics," *IEEE MTT-S Microwave Symposium Digest*, vol. 3, pp. 1633-1636, June 2003.

[5] Simion, S., "Modeling and design aspects of the MEMS switch," *International Semiconductor Conference2003,* vol. 1, pp. 125-128, 2003.

[6] Mercier, D., Blondy, P., Cros, D., Guillon, P., "An electromechanical model for MEMS switches," *IEEE Microwave Symposium Digest,* vol. 3, pp. 2123-2126, May 2001.

[7] Peroulis, D., Pacheco, S.P., Sarabandi, K., Katehi, L.P.B., "Electromechanical considerations in developing low-voltage RF MEMS switches," *IEEE Transactions on Microwave Theory and Techniques*, vol. 51, issue 1, pp. 259-270, Jan. 2003

[8] Bushyager, N., Lange, K., Tentzeris, M. and Papapolymerou, J., "Modeling and Optimization of RF-MEMS Reconfigurable Tuners with Computationally Efficient Time-Domain Techniques", *Proc. of the 2002 IEEE-IMS Symposium*, pp. 883-886, June 2002.

[9] Wang, Z., Jensen, B., Volakis, J., Saitou, K., Kurabayashi, K., "Analysis of RF-MEMS switches using finite element-boundary integration with moment method," *Antennas and Propagation Society International Symposium*, vol. 2, pp. 173-176, 22-27 June 2003.

[10] E.P. Popov, "Mechanics of Materials, Second Edition," Prentice-Hall, Inc, 1976.

[11] Stephen Senturia, "Microsystem Design," Kluwer Academic Publishers, 2001.

[12] James Gere, "Mechanics of Materials, Fifth Edition," Thompson-Engineering, 2003.

[13] Comsol, Inc. "FEMLAB Multiphysics Modeling," http://www.comsol.com/products/femlab/, November 2004.

[14] David Pozar, "Microwave Engineering, Second Edition," John Wiley & Sons, Inc., 1999.

[15] Muldavin, J. and Rebeiz, G., "High-Isolation CPW MEMS Shunt Switches – Part 1: Modeling," *IEEE Transactions on Microwave Theory and Techniques*, vol. 48, no. 6, pp. 1045-1052, June 2000.

[16] Qian, J., Li, G., deFlavis, F., "A parametric model of MEMS capacitive switch operating at microwave frequencies," *IEEE Microwave Symposium Digest*, vol. 2, pp. 1229-1232, June 2000.

Nickolas Kingsley received B.S. (2002) and M.S. (2004) degrees in electrical engineering from the Georgia Institute of Technology, where he is currently pursing a PhD. He is currently researching the integration and packaging of RF MEMS switches into various microwave devices on liquid crystal polymer (LCP) and silicon substrates. He is the recipient of the 2002 President's Undergraduate Research Award from Georgia Tech and the 2001 Armada Award from Compaq Computer Corporation. He is a student member of IEEE, IEEE APS, IEEE MTT-S, and Order of the Engineer.

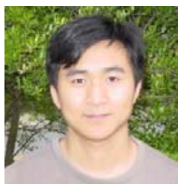

Guoan Wang received his Bachelor degree from Central South University, his Master of Science in Materials Science and Engineering from Zhejiang University, and his Master of Science in Electrical Engineering from Arizona State University. He is currently working toward the Ph.D degree in Electrical Engineering at the Georgia Institute of Technology. His research interests include: RF MEMS switches with novel materials and their applications for reconfigurable microwave circuits, integration of RF circuitry onto CMOS grade silicon, and micromachining techniques for microwave applications.

John Papapolymerou received the B.S.E.E. degree from the National Technical University of Athens, Athens, Greece, in 1993, the M.S.E.E. and Ph.D. degrees from the University of Michigan, Ann Arbor, in 1994 and 1999, respectively.

From 1999-2001 he was an Assistant Professor at the Department of Electrical and Computer Engineering of the University of Arizona, Tucson and during the summers of 2000 and 2003 he was a visiting professor at The University of Limoges, France. From 2001-2005 he was an Assistant Professor at the School of Electrical and Computer Engineering of the Georgia Institute of Technology, where he is currently an Associate Professor. His research interests include the implementation of micromachining techniques and MEMS devices in microwave, millimeter-wave and THz circuits and the development of both passive and active planar circuits on semiconductor (Si/SiGe, GaAs) and organic substrates (LCP, LTCC) for System-on-a-Chip (SOC)/ System-on-a-Package (SOP) RF front ends.

Dr. Papapolymerou received the 2004 Army Research Office (ARO) Young Investigator Award, the 2002 National Science Foundation (NSF) CAREER award, the best paper award at the 3rd IEEE International Conference on Microwave and Millimeter-Wave Technology (ICMMT2002), Beijing, China and the 1997 Outstanding Graduate Student Instructional Assistant Award presented by the American Society for Engineering Education (ASEE), The University of Michigan Chapter. His student also received the best student paper award at the 2004 IEEE Topical Meeting on Silicon Monolithic Integrated Circuits in RF Systems, Atlanta, GA. He has authored or co-authored over 120 publications in peer reviewed journals and conferences. He currently serves as the Vice-Chair for Commission D of the US National Committee of URSI and as an Associate Editor for IEEE Transactions on Antennas and Propagation. During 2004 he was the Chair of the IEEE MTT/AP Atlanta Chapter.